SOFT MODIFICATION AND FUNCTIONALIZATION OF LIGNOCELLULOSIC BIOMASS USED AS A LOW-COST EFFICIENT BIOSORBENT TO REMOVE BASIC FUCHSINE FROM AQUEOUS SOLUTION

SABRI MERADI,[*,**] CHAHRAZED DJILANI,[***,****] PIERRE MAGRI,[*****] YOUGHOURTA BELHOCINE[*,******] and FAYÇAL DJAZI[***,****]

[*]*Department of Process Engineering, Faculty of Technology, University 20 Août 1955, Skikda, Algeria*
[**]*Laboratory of Interactions, Biodiversity, Ecosystems and BIOTECHNology (LIBEB), University 20 Août 1955, Skikda, Algeria*
[***]*Faculty of Technology, University of 20 Août1955, El Hadaiek Road, B.O. 26 21000 Skikda, Algeria*
[****]*LRPCSI, University of 20 Août1955, El Hadaiek Road, B. O. 26 21000 Skikda, Algeria*
[*****]*LCP-A2MC, EA4164, University of Lorraine, 1, Blvd., Arago-57078 Metz, Cedex3, France*
[******]*Laboratory of Catalysis, Bioprocess and Environment, Department of Process Engineering, Faculty of Technology, University of 20 Août 1955, Skikda 21000, Algeria*
✉ *Corresponding author: S. Meradi, meradisabri21@gmail.com*

Received March 23, 2024

This study proposes a new modification of lignocellulosic biomass based on apricot kernel shells with composite activation KI/KOH and functionalized with a tolerant material (MgO) powder. Apricot kernel shells (NAK), modified apricot kernel shells (MAK) and doped apricot kernel shells (DAK) obtained were characterized using various methods, such as infrared spectroscopy (FTIR), scanning electron microscopy coupled with energy-dispersive X-ray spectroscopy (SEM-EDX), thermogravimetric analysis (TGA), X-ray diffraction (XRD), and point of zero charge (pH_{pzc}). The adsorbents were also evaluated in batch adsorption, using basic fuchsine dye (BF) to determine the performance and specific capacity of the adsorption process. The results showed that only 90 min and 0.1 g of DAK or MAK are sufficient to remove 93% and 91%, respectively, of basic fuchsine from aqueous solutions with a concentration of 20 mg/L in a volume of 100 mL. The MAK and DAK adsorbents can be reused for 5 cycles before their yield decreases below 50%, without requiring complex regeneration procedures, only drying for 4 h at 105°C. The evolution of adsorption was analyzed under different parameters, such as contact time, initial dose of adsorbent, initial dye concentration, initial pH, and temperature. The kinetic adsorption models indicate that the pseudo-second-order model was more suitable than the pseudo-first-order and intraparticle diffusion models for describing the adsorption process. The equilibrium adsorption data of BF were better fitted by the Langmuir isotherm, compared to the Freundlich and Temkin isotherms.

Keywords: synthesis, characterization, metal oxide, basic fuchsine, functionalization

INTRODUCTION

Nowadays, the intensive development in various sectors, such as industry and agriculture, and urban population growth are leading to numerous environmental problems.[1] The constantly increasing consumption of potable water, causing shortages, and the contamination of this vital resource are serious ecological issues.[2] According to the United Nations World Water Development Report, 2,000,000 tons of wastes are discharged into water bodies every day, including industrial wastes, dyes and chemicals.[3] Additionally, the continued population growth and diverse human activities have aggravated the scarcity of water resources. For instance, it is projected that billions of people worldwide will face water shortages by 2050.[4]

Dyes are among the most common pollutants, with over 10,000 different commercial dyes and pigments existing, and an annual production exceeding 700,000 tons. Dyes are extensively used in various industries, such as textiles, paper, printing, decoration, cosmetics, pharmaceuticals, histology, food processing, rubber and plastics.[3,5,6] Dyes are polyaromatic molecules, containing at least one unsaturated compound (chromophore) and a functional group (auxochrome).[7] The complex cyclic and large structures of dyes make them more persistent in the aquatic environment, and they are more difficult to filter from wastewater.[8] Water contaminated with dyes is unsuitable for drinking and other purposes because of its high toxicity; dyes can cause cancer, dermatitis, provoke allergies, and contribute to other diseases.[9,10] Several methods have been widely used to degrade or remove organic pollutants such as dyes, pesticides, polycyclic aromatic hydrocarbons and metal ions. These technical processes include microbiological degradation,[11] coagulation-flocculation,[12] chemical oxidation, reverse osmosis, micro and ultrafiltration,[13] electrochemical treatment, photocatalytic degradation,[14,15] sonocatalytic degradation[16] and adsorption.[6] The adsorption method has been widely employed for dye removal from wastewater, mainly due to its superior effectiveness compared to other techniques, which are often limited by various factors. This approach relies on the adsorption of a dye onto a surface coated with a thin layer of porous adsorbent; the porous structure and functional sites on the surface of the adsorbent are used to remove pollutants from the wastewater. This method is widely preferred due to its effective treatment with low cost and eco-friendly operational simplicity.[17]

The shell of apricot kernels is a valuable residue resulting from food production and processing. It contains numerous pores on its surface and inside,[18] making it an ideal porous biomass adsorbent material. These properties characterize it as an excellent low-cost absorbent for removing pollutants from wastewater.

This study focuses on developing and characterizing apricot kernel shell as an eco-friendly biomass adsorbent prepared with environmentally tolerant products and at very low energy consumption. The results revealed the high performance of the adsorbent evaluated in batch adsorption of basic fuchsine. Additionally, the adsorption process was investigated to determine its kinetic and equilibrium isotherm models.

EXPERIMENTAL

Preparation and synthesis of MAK and DAK

The biomass wastes were obtained from a basic oil extraction unit, and denoted as natural apricot kernels (NAK). Initially, the biomass was washed, ground using a mill, and sieved to obtain particles with a diameter less than 1 mm. This material was then modified with a composite chemical activation solution (KI/KOH), at various ratios, for 90 min, to facilitate preliminary applications in the removal of basic fuchsine and to evaluate the most effective ratio.

In a subsequent stage, the materials were doped with magnesium oxide (DAK). 2 g of magnesium oxide was dissolved in 150 mL solution of distilled water containing 1% acetic acid. Subsequently, 10 g of the modified material was added to this solution and kept under moderate agitation at 80 °C for 1 h. Afterward, the pH of the solution was carefully adjusted to pH 10 and left under agitation for an additional 3 h at 80 °C .

Characterization of MAK, NAK and DAK

These materials underwent several characterization techniques. Fourier transform infrared spectroscopy (FTIR) analysis was conducted using a Bruker Invenio R spectrometer (350 and 4000 cm^{-1}) to identify surface functional groups. Scanning electron microscopy with energy dispersive X-ray analysis (SEM/EDX), using a Thermo Scientific PV25MK instrument (Great Britain), was employed to examine morphology and elemental composition differences. Thermal gravimetric analysis (TGA), performed with a Mettler Toledo apparatus from Quantachrome Instruments (USA), allowed continuous recording of sample mass changes with temperature increase. The study of crystalline material phases was enabled by X-ray diffraction (XRD) analysis, conducted with a Malvern Panalytical B.V. instrument from Lelyweg, Netherlands. The point of zero charge (pH_{pzc}) was determined using a method proposed by Adam.[19] A series of 50 mL NaCl 0.01 M solutions were prepared, and their pH was adjusted from 2 to 12 using 0.01 M solutions of HCl or NaOH. Upon achieving a constant pH value, 0.15 g of biomass was added to each flask, sealed, and placed in a shaker for three days. The pH_{pzc} value represents the point where the pH_{final} vs $pH_{initial}$ curve intersects the line $pH_{initial}$= pH_{final}.

Batch adsorption experiments

The adsorption experiments were performed using solutions of basic fuchsine (molecular formula: $C_{20}H_{20}N_3Cl$, molecular weight: 337.86 g mol^{-1}). Dye solutions were prepared using distilled water, with a stock solution of BF (1.0) g/L stored in an amber flask. Adsorption experiments utilized dilute solutions derived from this stock.

Equilibrium adsorption studies were conducted at temperatures of 30 °C, 40 °C, and 50 °C, using the optimal pH determined from preliminary adsorption studies, where values of pH 2, pH 4, pH 5, pH 6.6 and pH 8 were investigated. The initial dye concentration ranged from 5 to 100 mg/L. Specifically, equilibrium adsorption data were collected at pH 6.6. All batch adsorption experiments were performed using a thermostatic multi-stirrer.

The concentration of the colored solution was determined by measuring absorbance using a UV-Vis spectrophotometer (Shimadzu UV-1700) at a wavelength of 546 nm to assess residual BF concentration.

The quantity of retained dye at equilibrium q_e (mg/g) was calculated by the following expression:

$$q_e(mg/g) = \frac{(C_i - C_e).V}{W} \quad (1)$$

The dye percent retained at the equilibrium was calculated by the following equation:

$$R(\%) = \frac{(C_i - C_t)}{C_i} \times 100 \quad (2)$$

The amount of dye absorbed by the material (q_t) at time t was calculated by:

$$q_t(mg/g) = \frac{(C_i - C_t).V}{W} \quad (3)$$

where C_i (mg/L) is the initial concentration of the dye in solution, C_t (mg/L) is the dye concentration in solution at any time, V is the volume of the solution in L, W is the mass of MAK and DAK expressed in g.

Kinetic and isotherm study

The adsorption kinetics of BF by MAK and DAK were evaluated using three common models: pseudo-first-order, pseudo-second-order, and intraparticle diffusion models.

Pseudo-first-order equation:

$$Ln(q_e - q_t) = Ln(q_e) - k_1 t \quad (4)$$

Pseudo-second-ordre equation:

$$\frac{t}{q_t} = \frac{1}{k_2 q_e^2} + \frac{1}{q_e} t \quad (5)$$

Intraparticle diffusion equation:

$$q_t = k_{int}^{0.5} + C \quad (6)$$

The adsorption isotherms were analyzed using the Langmuir, Freundlich, and Temkin models.

Langmuir isotherm equation:

$$\frac{1}{q_e} = \frac{1}{q_{max}} + \frac{1}{K_L \cdot q_{max}} \times \frac{1}{C_e} \quad (7)$$

Freundlich isotherm equation:

$$lnq_e = lnK_f + \frac{1}{n} lnC_e \quad (8)$$

Temkin isotherm equation:

$$q_e = \frac{RT}{B_T} lnA_T + \left(\frac{RT}{B_T}\right) lnC_e \quad (9)$$

RESULTS AND DISCUSSION

Characterization of natural, modified and doped apricot kernel shells

Infrared spectroscopy

The distribution of functional groups on the surfaces of NAK, MAK, and DAK, before and after adsorption, was analyzed using FTIR spectroscopy. Figure 1 illustrates that apricot kernel biomass modified with KI/KOH and doped with magnesium oxide contains several functional groups. The broad and intense band observed at 3020-3605 cm^{-1} corresponds to the O-H stretching of alcohol groups associated with hemicelluloses, cellulose and lignin.[20] The peak at 2890 cm^{-1} represents the antisymmetric stretching vibration of C-H bonds in methyl groups (CH_3), while stretching vibrations at 1620-1690 cm^{-1} indicate the presence of -C-O- amide bonds. Additionally, the absorption bands at 1319 cm^{-1} and 1481 cm^{-1} suggest the presence of alkyl groups (-CH_3, -CH_2, and -CH), characteristic of cellulose, hemicelluloses, and lignin compositions. The peaks at 932 cm^{-1} and 1160 cm^{-1} correspond to C-O-C and C-O-H stretching in cellulose, while those at 660 and 520 cm^{-1} are assigned to C-N stretching and other cellulose-related groups.[18]

Comparative FTIR analysis of NAK, MAK, and DAK confirms that there were no changes in the functional groups after composite activation of NAK with KI/KOH and functionalization of MAK with magnesium oxide. However, there are clear differences in intensity at all characteristic peaks and bands. For instance, the intensity of the O-H band was 86.08%, 91.66%, and 53.06% for NAK, MAK, and DAK materials, respectively.

The spectrum of MAK before adsorption shows identical functional groups, with an increase in intensity observed after adsorption. In contrast, the spectrum of DAK before adsorption is more intense than the spectrum after adsorption, possibly due to the well-covered surface and the formation of strong bonds between DAK and BF. The FTIR analysis suggests that the adsorption of BF onto DAK adsorbent forms stronger bonds compared to the adsorption of BF onto MAK adsorbent.

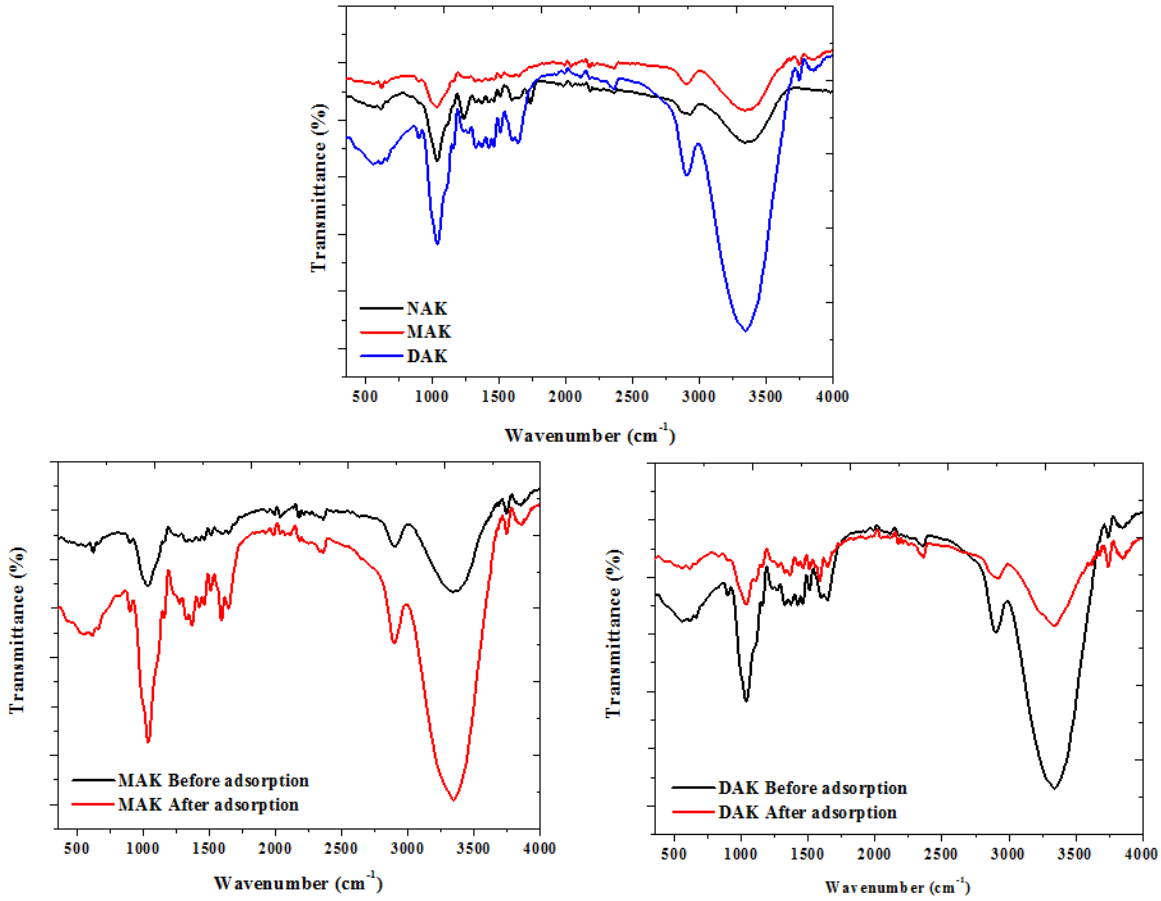

Figure 1: FTIR spectra of NAK, MAK, DAK, MAK-BF dye and DAK-BF dye

Scanning electron microscopy

Scanning electron microscopy (SEM) is one of the most versatile methods for the examination and analysis of the microstructure, chemical composition and physical (size and shape) characterizations. Figure 2 displays the SEM photographs of NAK, prepared MAK, and DAK samples before and after adsorption. From the SEM images of NAK, numerous pores can be detected. As shown in Figure 2 (MAK and DAK), the surfaces of MAK and DAK exhibit comparatively rough textures, with intertwined cavities that occupy a large surface area. The SEM images also confirm the successful treatment of MAK with KI/KOH and the functionalization of DAK with MgO. It is evident that the pores of MAK and DAK powder were covered by the BF dye after adsorption (Fig. 2).

Energy dispersive X-ray spectroscopy

Table 1 presents the results of the elemental composition analysis of the adsorbent materials NAK, MAK, and DAK, performed using EDX equipment. The majority of the composition consists of carbon and oxygen, which is characteristic of the natural origin of apricot kernels. The presence of magnesium, at 2.66% in the DAK material, confirms the successful functionalization of the biomass with the mineral oxide MgO used, demonstrating an effective and soft preparation technique for doped materials.

Table 1
Elemental composition of samples

Adsorbents	Atomic (%)						
	C	O	Al	Mn	Mo	I	Mg
NAK	53.28	45.10	0.49	0.90	0.07	0.17	-
MAK	76.79	14.58	-	-	-	8.63	-
DAK	51.23	43.69	-	-	-	2.41	2.66

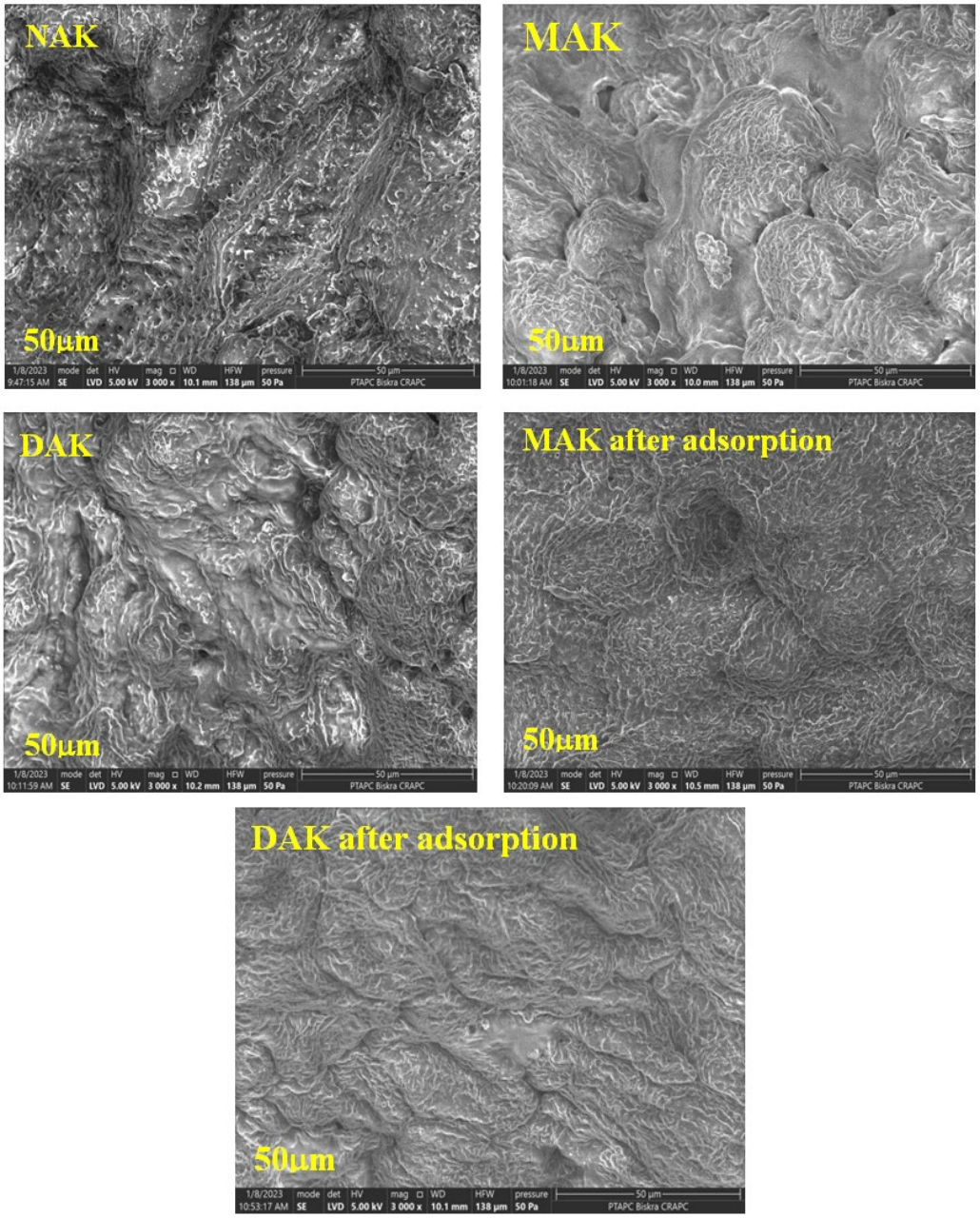

Figure 2: SEM images of NAK, MAK, DAK, MAK-BF dye and DAK-BF dye

Thermal analysis

The TGA and DTG curves illustrating the thermogravimetric analysis of NAK, MAK, and DAK are clearly depicted in Figure 3. The weight loss occurs in three significant stages, which are similar for NAK and MAK, with slight variations observed in DAK. The first stage shows a mass loss of 5.95%, 5.94%, and 7.71% for NAK, MAK, and DAK, respectively, occurring at temperatures of 82.21 °C, 82.52 °C, and 87.04 °C. This corresponds to the removal of adsorbed water molecules from the surface of the biomass. The second stage exhibits a mass loss of 31.75% and 27.19% for NAK and DAK, respectively, at temperatures of 295.09 °C and 293.24 °C. This stage is indicative of the initial degradation of lignin.[21] The third stage, occurring at temperatures of 357.35 °C and 359.10 °C for NAK and DAK, respectively, involves a mass loss of 30.28% and 30.15%. This stage is associated with the decomposition of cellulose and hemicelluloses.[22] In contrast, DAK exhibits a distinct second stage

at 333.51 °C with a mass loss of 53.25%, indicating degradation within the range of lignin, cellulose, and hemicellulose components. Above 450 °C, carbonization of the biomass occurs, with no significant weight loss observed after 776 °C. This confirms the formation of fixed carbon percentages of approximately 20%, 19%, and 21% for NAK, MAK, and DAK, respectively.

X-ray diffraction

Figure 4 shows the XRD patterns of the adsorbents used and MgO. The analysis revealed two typical peaks at 22° and 34°, consistent with previous studies, with a slight shift in 2θ attributed to contributions from the NAK material: from 21.98° to 22° and from 36.28° to 34°. The peak at 22° is associated with amorphous carbon, while the smaller peak at 34° is attributed to the crystalline structure of cellulose,[23] indicative of the presence of (004) lattice planes and hydrogen bonding within and between molecules, resulting in an ordered crystalline arrangement. All materials, NAK, MAK, and DAK, exhibit similar typical peaks with increasing crystallinity values of 9.9%, 10.17%, and 12.13%, respectively. These values suggest that activation with KI/KOH and functionalization with magnesium oxide influenced the morphology of NAK. Concerning the XRD pattern of MgO, two strong peaks are observed at 43.06° and 62.44°, with smaller peaks preceding these at 37.11° and 58.89°, indicating the semi-crystalline structure characteristic of magnesium oxide, with a crystallinity of approximately 55.55%.

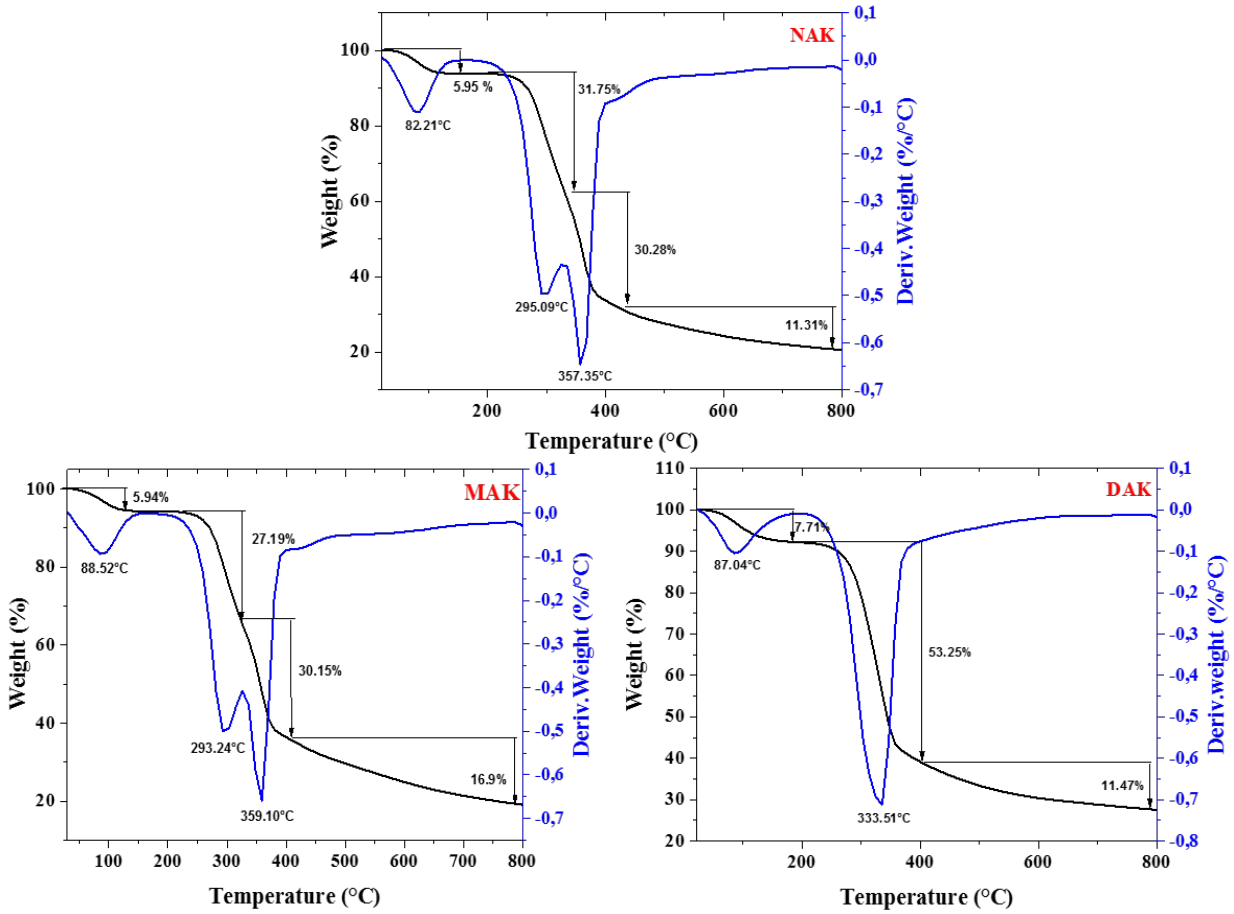

Figure 3: TGA/DTG analysis of NAK, MAK and DAK

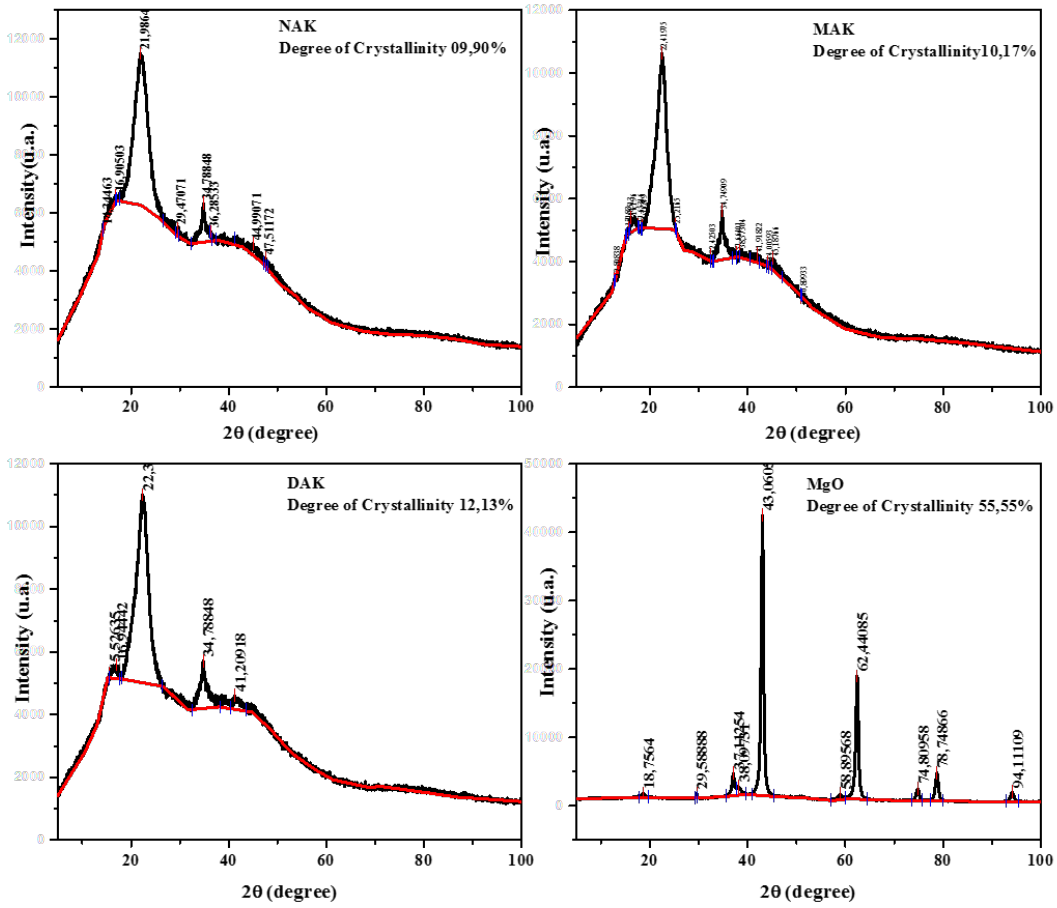

Figure 4: X-ray diffraction patterns of NAK, MAK, DAK and MgO samples

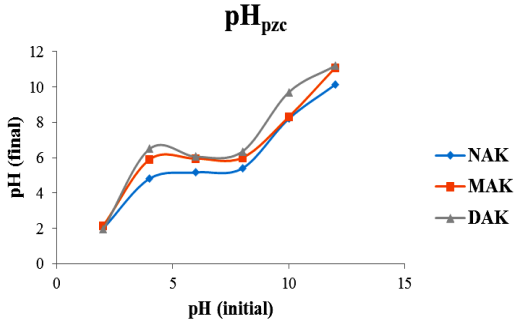

Figure 5: pH point of zero charge (pH_{pzc}) of NAK, MAK and DAK

Point of zero charge pH_{pzc}

The point of zero charge is typically defined as the pH at which the net charge on the total particle surface equals zero.[24] The pH_{pzc} was determined using a simple electrochemical method, as depicted in Figure 5, with the experimental results. The pH_{pzc} is identified where the curve of $pH_{initial}$ vs. pH_{final} intersects the line pH_{final}= $pH_{initial}$, yielding values of 5 for NAK, and 6 for both MAK and DAK. Experimental data confirm that NAK, MAK, and DAK exhibit acidic properties. Specifically, NAK demonstrates stronger acidity compared to MAK and DAK, which exhibit moderate acidic properties. The pH_{pzc} determines the point where the adsorbent surface transitions from a net positive charge at pH < pH_{pzc} to a net negative charge at pH > pH_{pzc}.[25]

A pH_{pzc} of 6 for MAK and DAK indicates that the adsorbent surfaces are positively charged at pH values below 6 and negatively charged at pH values above 6. As pH approaches pH_{pzc}, the

density of positive ions on the adsorbent surface increases,[26] leading to a repulsive effect due to excess positively charged ions in the solution. This phenomenon is reflected in the adsorption behavior of BF molecules: in strongly acidic conditions (pH 2), there is minimal binding of BF molecules due to neutralization of charges, thereby reducing the electrostatic attraction and consequently, the adsorption capacity. Maximum adsorption of BF on MAK and DAK is achieved above pH_{pzc}, where the prevalence of negative charges enhances the electrostatic attraction to BF anions, facilitating their adsorption.

Preliminary tests

We assessed the efficiency of apricot kernels to remove BF in its natural state (NAK) and modified (MAK) with a composite chemical activation of KI/KOH in various ratios. At 90 minutes, under identical operating conditions, apricot kernel biomass prepared with a 0.5/0.5 (KI/KOH) ratio exhibited the best performance. All subsequent experiments were conducted using the 0.5/0.5 ratio. The biomass modified with KI/KOH (0.5/0.5) was further doped with magnesium oxide to enhance BF adsorption performance. BF adsorption was tested using both MAK and DAK to observe differences in removal efficiency (Fig. 6).

Effects of various parameters influencing the adsorption

Effect of adsorbent mass

The adsorbent mass is a fundamental parameter for evaluating optimal conditions to achieve the highest removal efficiency of BF. The increase in adsorbed amount of BF is proportional to the adsorbent mass. This relationship is logical because a greater mass of adsorbent provides a larger specific adsorption area. The highest adsorption efficiency is achieved with an adsorbent mass of 0.1 g for both MAK (91.62%) and DAK (93.34%). The evolution of qt (mg/g) indicates that BF adsorption occurs in a multilayer mode with both MAK and DAK (Fig. 7).

Effect of initial dye concentration

The initial dye concentration significantly influences the performance and adsorption capacity of the used adsorbents. Figure 8 illustrates the effect of different initial concentrations of BF dye (5, 10, 20, 50, and 100 mg/L) on the batch adsorption of both MAK and DAK. The experimental conditions, such as pH of the solution, 0.1 g of adsorbent mass, agitation speed, and temperature were kept constant.

The adsorption of BF dye by DAK material consistently showed higher performance and capacity, compared to MAK, throughout all experiments. The maximum removal efficiencies of BF dye from solutions with an initial concentration of 5 mg/L were 98.68% for DAK and 97.28% for MAK.

Effect of initial pH

The initial pH of the solution significantly influences the surface charge of the adsorbent and the ionization degree of dyes or elements present in the solution. Hydroxyl and hydrogen ions can alter the charge of elements in solution, shifting them towards a zero charge point, thereby impacting the performance of adsorption.

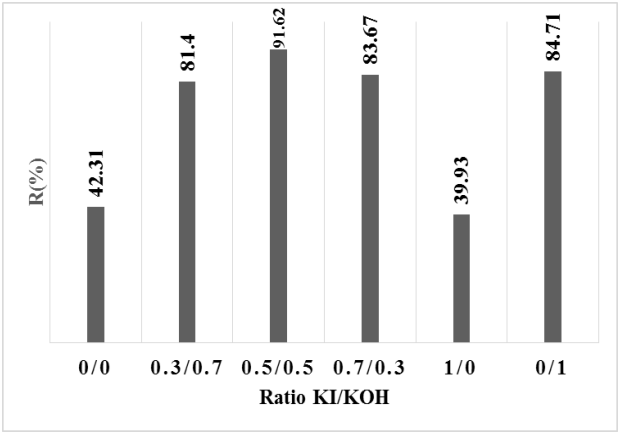

Figure 6: Effect of different ratios of composite activator (KI/KOH) (adsorption conditions: 1 g/L of MAK, initial concentration of BF 20 mg/L, pH 6.6 and t = 90 min)

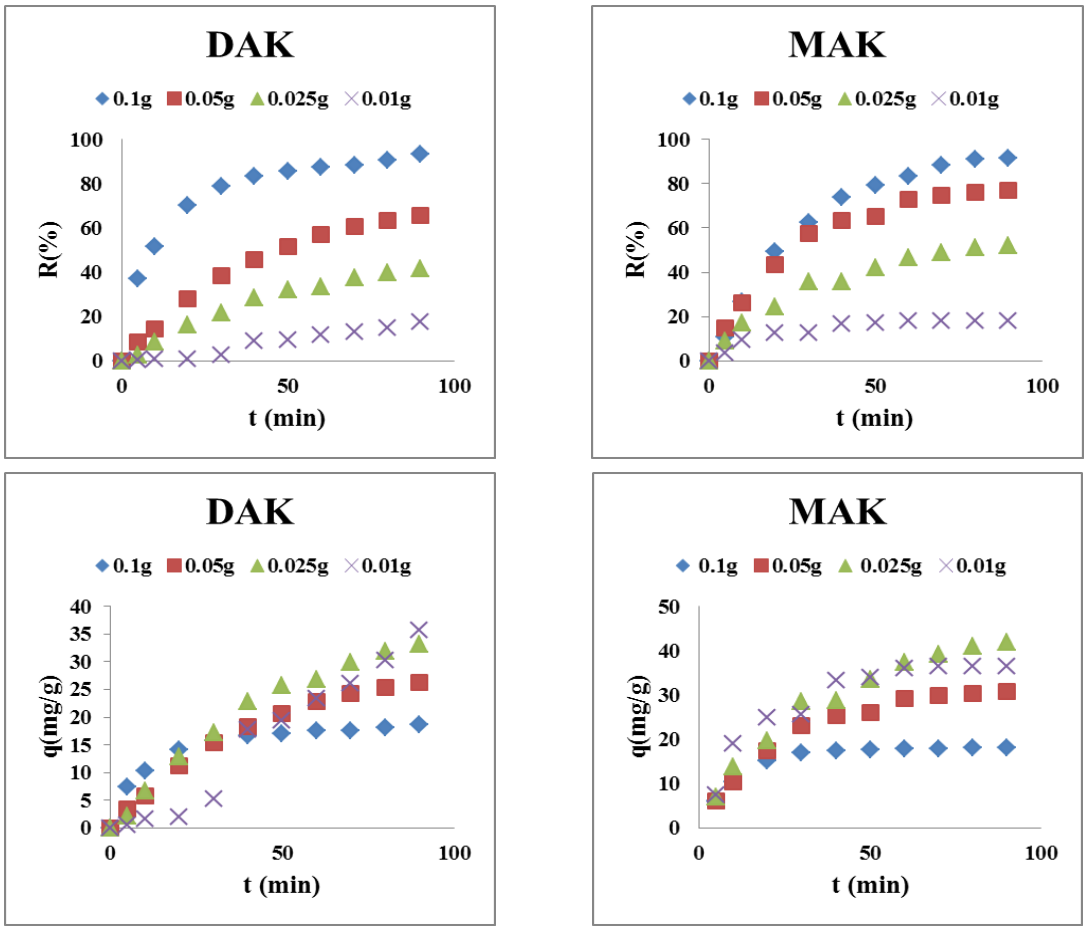

Figure 7: Effect of adsorbent mass (MAK and DAK) on removal of BF (adsorption conditions: 0.1-1 g/L of MAK or DAK, initial concentration of BF 20 mg/L, pH 6.6)

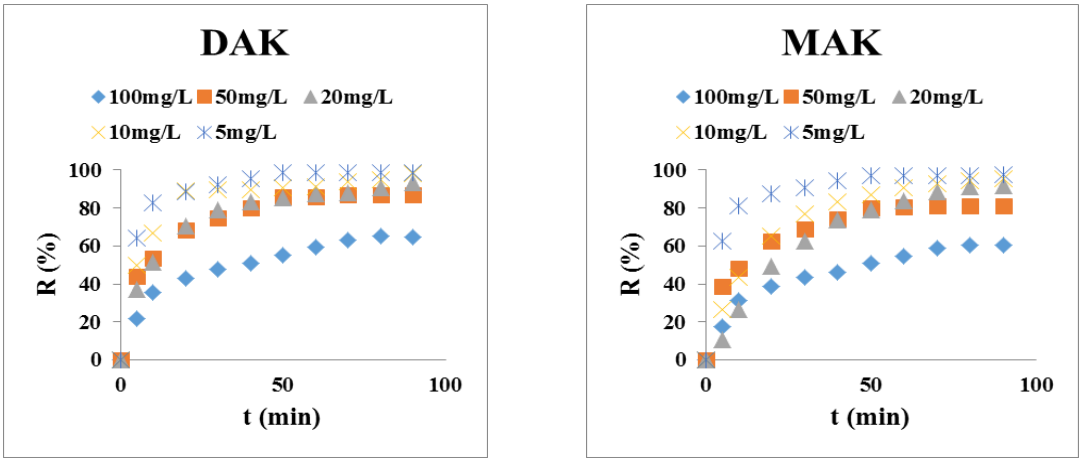

Figure 8: Effect of different initial concentrations of BF dye on its adsorption onto MAK and DAK (adsorption conditions: 1 g/L of MAK or DAK, initial concentration of BF 5-100 mg/L, pH 6.6)

Different pH values ranging from 2 to 8 were tested to observe their effects. The mass of adsorbent, temperature, agitation speed, and initial concentration of BF were kept constant at 0.1 g, 22 °C, 240 rpm, and 20 mg/L, respectively. As shown in Figure 9, the evolution of adsorption at different pH values showed that the removal percentage and the amount of BF adsorbed on MAK increased proportionally with increasing pH, particularly up to pH 7. At pH 8, there was a decrease in both removal percentage and amount adsorbed, possibly due to the basic nature of the

solution neutralizing the surface charge of the adsorbent and occupying positively charged functional sites that attract basic fuchsine.

In contrast, the adsorption behavior of DAK adsorbent was notably different. The removal percentage and the amount adsorbed were relatively similar at pH 2, pH 4, and pH 5. This is likely due to the presence of magnesium on the surface of the doped adsorbent, which influences ionic forces affecting adsorption mechanisms in acidic solutions. The removal percentage and amount adsorbed increased again at pH 6.6 and pH 8. This pH effect demonstrates the changes that occurred on the adsorbent surface after functionalization with magnesium oxide.

Effect of temperature

The effect of solution temperature is a critical parameter in batch adsorption. Figure 10 illustrates the adsorption of BF onto MAK and DAK adsorbents at various temperatures (30, 40, and 50 °C). The other experimental parameters, such as pH of the solution, 0.1 g of adsorbents, agitation speed and initial concentration, were kept constant. The amount of BF adsorbed increases consistently with rising temperature. Higher temperatures enhance the kinetics of the adsorption process, resulting in greater adsorption. This indicates that the overall adsorption process is endothermic in nature.[20]

Thermodynamics of adsorption

The feasibility and characteristics of the adsorption process of BF dye on MAK and DAK were evaluated using thermodynamic parameters: standard Gibbs free energy change (ΔG° in $kJ.mol^{-1}$), enthalpy change (ΔH° in $kJ.mol^{-1}$), and entropy change (ΔS° in $kJ.mol^{-1}·K^{-1}$).

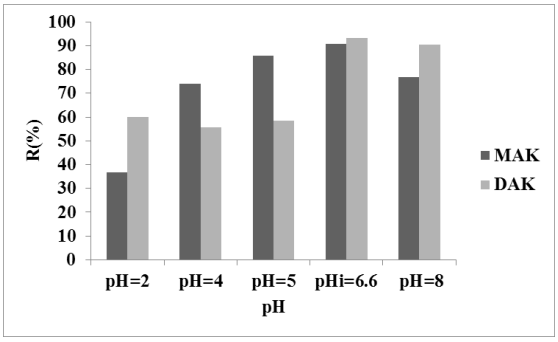

Figure 9: Effect of initial solution pH on removal of BF by MAK and DAK (adsorption conditions: 1 g/L of MAK or DAK, initial concentration of BF 20 mg/L, pH=2-8, t = 90 min)

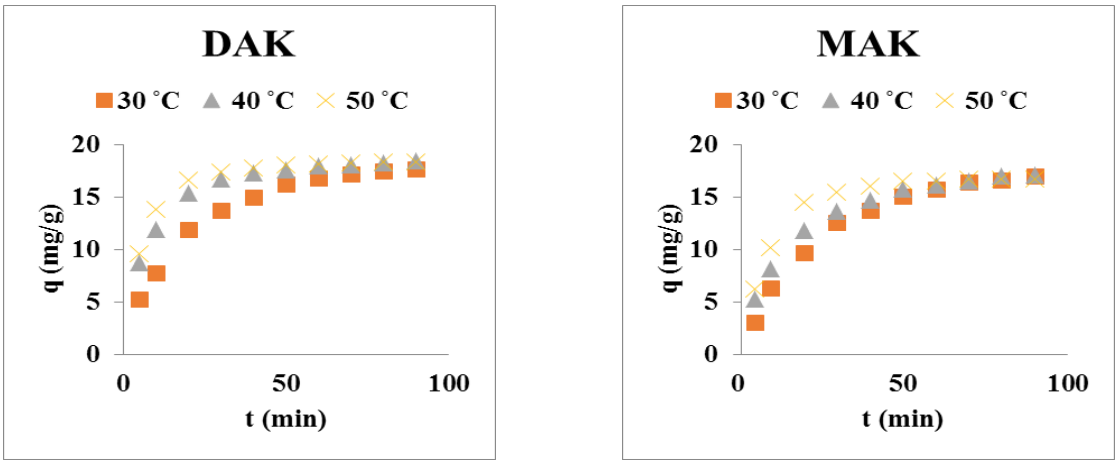

Figure 10: Effect of temperature on adsorption of BF onto MAK and DAK adsorbents (adsorption conditions: 1 g/L of MAK or DAK, initial concentration of BF 20 mg/L, pH 6.6)

Table 2
Thermodynamic parameters of MAK and DAK adsorbents

Adsorbents	T (°K)	ΔG° (kJ.mol^{-1})	ΔH° (kJ.mol^{-1})	ΔS° (kJ.mol^{-1}.K^{-1})
MAK	303	-4.422	0.689	0.168
	313	-4.593		
	323	-4.760		
DAK	303	-5.116	25.576	0.101
	313	-6.434		
	323	- 7.135		

The standard free energy change of the adsorption process was calculated using the Van't Hoff[27] equation:

$$K_D = \frac{q_e}{C_e} \quad (10)$$

$$lnK_D = \frac{\Delta S^\circ}{R} - \frac{\Delta H^\circ}{RT} \quad (11)$$

$$\Delta G^\circ = \Delta H^\circ - T\Delta S^\circ \quad (12)$$

$$\Delta G^\circ = -RT\ Ln\ K_D \quad (13)$$

where K_D is the distribution factor, R (8.314 J.mol^{-1}.K^{-1}) is the universal gas constant and T is the temperature in Kelvin. The ΔH° and ΔS° were estimated from experimental data. The distinction between chemisorption and physical adsorption bonds relies on the enthalpy change magnitude. Typically, bonds weaker than 84 kJ.mol^{-1} indicate physical adsorption, while chemisorption bonds range from 84 to 420 kJ.mol^{-1}.[19] From our findings, ΔG° was negative and ΔH° was positive, indicating spontaneous, favorable, and endothermic adsorption. The higher ΔH° for DAK, compared to MAK, suggests that DAK exhibits greater potential, reactivity, and performance.[28,29] The positive ΔH values confirm the endothermic nature of adsorption, indicating that energy is required for the process.

Adsorption kinetics modelling

Kinetic studies have been employed to describe the mechanisms of BF dye adsorption on MAK and DAK adsorbents by examining the dynamics of mass transfer and the equilibrium reaction time in terms of the order of rate constants.[30] The experimental data were simulated using first-order, second-order and intraparticle diffusion models. Table 3 presents the fitting parameters R^2, k_1, k_2, k_{int}, and $q_{e,cal}$ for the adsorption of basic BF by MAK and DAK. The adsorption dynamics of BF dye on MAK and DAK show better agreement with the second-order model, compared to the first-order and intraparticle diffusion models. The R^2 values for the second-order model consistently exceeded 0.930 in all experiments for both MAK and DAK. However, the R^2 values obtained from the intraparticle diffusion kinetic model ranged from 0.521 to 0.871 for MAK and from 0.518 to 0.847 for DAK.

The pseudo-second-order kinetic model approach suggests that the adsorption of BF dye onto MAK and DAK adsorbents was governed by chemisorption, involving valence forces through the sharing or exchange of electrons between the adsorbent and the adsorbate.[31]

For a comprehensive evaluation of the BF dye adsorption process, the intraparticle diffusion model was investigated at various initial concentrations. Thus, according to the intraparticle diffusion model, when qt is plotted as a function of $t^{0.5}$, the plots depict a linear relationship between qt and $t^{0.5}$, revealing three distinct stages observed across various concentration experiments (plots not shown). These stages govern the adsorption of BF onto MAK and DAK: the first stage involves external mass transfer between the adsorbent material and BF dye, followed by the diffusion of the adsorbed molecules into the adsorbent particles. The final stage occurs when adsorption reaches equilibrium.

Adsorption isotherms

The adsorption isotherm models the relationship between the concentration of the adsorbate and its degree of adsorption onto the adsorbent surface at a constant temperature.[32] The Langmuir, Freundlich and Temkin adsorption isotherms models are employed to describe the equilibrium adsorption data of BF dye, as presented in Table 4.

Table 3
Parameters of the kinetic models for the adsorption of BF onto MAK and DAK

Model		Pseudo-first-order				Pseudo-second-order			Intraparticle diffusion	
	C_0 (mg/L)	$q_{e,exp}$ (mg/g)	$q_{e,cal}$ (mg/g)	k_1 (min^{-1})	R^2	$q_{e,cal}$ (mg/g)	$k_2 \times 10^{-4}$ ($g.mg^{-1}min^{-1}$)	R^2	k_{int} ($mg/g.min^{1/2}$)	R^2
MAK	5	4.86	3.98	0.03	0.830	5.05	710	0.999	0.32	0.521
	10	9.54	0.97	0.03	0.980	11.24	50	0.999	0.87	0.815
	20	18.36	0.29	0.03	0.986	29.41	7.3	0.939	1.91	0.900
	50	40.68	1.77	0.01	0.857	45.45	28	0.998	3.29	0.726
	100	60.31	0.75	0.01	0.944	71.43	8.2	0.991	5.42	0.871
DAK	5	4.93	3.72	0.04	0.876	5.13	712	0.999	0.32	0.518
	10	9.78	2.80	0.03	0.848	10.10	211.6	0.998	0.69	0.601
	20	18.67	1.16	0.23	0.954	20.41	53	0.999	1.09	0.790
	50	43.46	2.04	0.02	0.871	47.62	30	0.998	3.41	0.704
	100	64.87	0.91	0.01	0.947	76.92	8.8	0.991	5.63	0.847

Table 4
Parameters of isotherm models for the removal of BF onto MAK and DAK

Adsorbents	MAK	DAK
Langmuir isotherm		
q_{max} (mg/g)	66.67	71.43
K_L(L/g)	3.46	2.36
R^2	0.992	0.992
Freundlich isotherm		
K_f	7.02	7.68
n	0.45	0.41
R^2	0.987	0.986
Temkin isotherm		
B_T	10.01	9.69
K_T	6.96	13.87
R^2	0.944	0.921

The R^2 values obtained from the adsorption models indicate that the three isotherms provide a good fit for the adsorption of BF dye on MAK and DAK adsorbents materials. Still, the Langmuir model was found to be more compatible with the adsorption of BF dye compared to the Freundlich and Temkin models. The maximum adsorption capacities of DAK and MAK adsorbents for BF dye were 71.43 mg/g and 66.67 mg/g, respectively. The K_L value of MAK adsorbent was higher than that of DAK, suggesting that MAK may require a higher adsorption energy, which indicates stronger dynamic forces influencing the adsorption mechanism.

Adsorbent reuse

MAK and DAK materials were reused for several cycles to assess the reusability of these adsorbents. After each cycle, the adsorbents were dried for 4 h at 105 °C and then reused for subsequent adsorption cycles until the removal efficiency of BF decreased to less than 50%. The DAK adsorbent consistently showed higher efficiency than the MAK adsorbent until the sixth cycle, where both achieved the same percentage of BF dye removal: 41.17% for MAK and 41.25% for DAK. This similarity may be attributed to the surface area being covered by multiple layers of dye, which reduces the ionic effect of the impregnated magnesium. The performance difference in adsorption confirms that enhancing the material with magnesium oxide makes the adsorbent more effective in the first five cycles of reuse, without requiring rigorous regeneration conditions (Fig. 11).

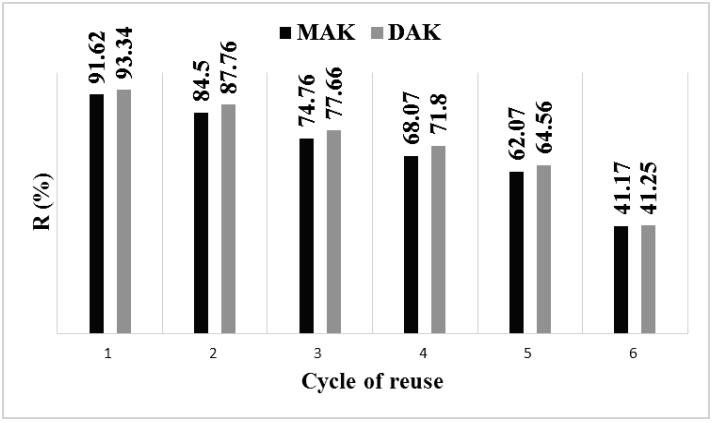

Figure 11: Number of reuse cycles for MAK and DAK in removing BF

Table 5
Comparison of different adsorbents based on BF dye adsorption capacity ($mg.g^{-1}$)

Adsorbents	Dye	q_{max}(mg/g)	References
Chicken bones	BF	112.79	[29]
Magnetic NaY zeolite	BF	2.026	[33]
Kaolin–chitosan composite	BF	7.11	[34]
XG/CFLO	BF	36.23	[35]
TiO_2/MWCNTs	BF	32.05	[36]
Gum-PVP/SiO_2	BF	16.33	[37]
Gum-PVP/SiO_2-magnetic	BF	91.49	[37]
Cation-exchange resin	BF	113.7	[28]
$MnFe_2O_4$/DE-NaOH	BF	274.73	[5]
Cellulose modified with maleic anhydride	BF	31.92	[38]
MAK	BF	66.66	This study
DAK	BF	71.42	This study

Comparison of maximum adsorption capacities of BF dye by various adsorbents

The comparative effectiveness of MAK and DAK was assessed in conjunction with various studies. Table 5 outlines the maximum adsorption capacities of different materials utilized for the removal of BF dye. As observed from Table 5, MAK and DAK exhibit significant adsorption capacities compared to other adsorbents, highlighting the

cost-effectiveness and eco-friendly nature of preparing adsorbents from natural apricot kernel shells, which are readily available in abundance.

CONCLUSION

This study focuses on the technical development and valorization of biomass lignocellulosic materials. The investigated adsorbents, MAK and DAK, were utilized to effectively remove basic fuchsine dye from wastewater, demonstrating efficient performance within a short timeframe. This achievement is facilitated by using soft products and employing a gentle preparation method. Specifically, using only 0.1 g of either DAK or MAK for a duration of 90 min was sufficient to achieve 93% and 91% removal, respectively, of basic fuchsine from aqueous solutions initially containing 20 mg/L in 100 mL.

The maximum adsorption capacities of basic fuchsine dye were found to be 66.66 mg/g for MAK and 71.42 mg/g for DAK. The adsorption process was influenced by various factors, such as contact time, adsorbent dose, initial dye concentration, initial pH of the solution, and temperature. The investigated adsorbents maintained their effectiveness through 5 cycles of reuse, retaining efficiency above 50%, without needing rigorous regeneration, only requiring drying for 4 h.

The kinetics of adsorption were best described by the pseudo-second-order model, which showed better fit compared to the pseudo-first-order model and intraparticle diffusion. The equilibrium adsorption data for basic fuchsine were best fitted by the Langmuir model, followed by the Freundlich and Temkin models.

Overall, the experimental results demonstrate that this gentle and cost-effective method of valorizing agricultural residues yields biosorbents that can effectively remove dyes from wastewater, highlighting their potential for practical application.

REFERENCES

[1] S. Jia, J.-M. Yu, L. Zhai, C. Yang, T. Yang *et al*., *J. Solid State Chem*., **324**, 124100 (2023), https://doi.org/10.1016/j.jssc.2023.124100

[2] F. Zhou, W. Zhang, A. Jiang, H. Peng, L. Li *et al*., *Ecol. Indic*., **154**, 110874 (2023), https://doi.org/10.1016/j.ecolind.2023.110874

[3] M. Sulyman, J. Namieśnik and A. Gierak, *Eng. Prot. Environ*., **19**, 611 (2016), https://doi.org/10.17512/ios.2016.4.14

[4] C. Ren, Y. Wang, L. Yu, H. Zhang and Z. Xie, *J. Environ. Manage*., **345**, 118882 (2023), https://doi.org/10.1016/j.jenvman.2023.118882

[5] Z. Sun, G. Yao, M. Liu and S. Zheng, *J. Taiwan Inst. Chem. Eng*., **71**, 501 (2017), https://doi.org/10.1016/j.jtice.2016.12.013

[6] E. Mounra, A. Malloum, J. J. Fifen and J. Conradie, *J. Mol. Model*., **29**, 380 (2023), https://doi.org/10.1007/s00894-023-05761-8

[7] C. O. Aniagor, A. Hashem, N. M. Badawy and A. A. Aly, *Hybrid Adv*., **3**, 100047 (2023), https://doi.org/10.1016/j.hybadv.2023.100047

[8] R. Tohamy, S. S. Ali, F. Li, K. M. Okasha, Y. A.-G. Mahmoud *et al*., *Ecotoxicol. Environ. Safet*., **231**, 113160 (2022), https://doi.org/10.1016/j.ecoenv.2021.113160.

[9] A. Mehdinia, S. M. Sadat Shilsar and S. Mozaffari, *J. Iran. Chem. Soc*., **20**, 1073 (2023), https://doi.org/10.1007/s13738-022-02732-3

[10] S. A. Mohammed, O. S. A. Al-Khazrajy, M. Abdallh, K. A. Aadim, A. Al-Mamari *et al*., *Environ. Process*., **10**, 63 (2023), https://doi.org/10.1007/s40710-023-00677-0

[11] H. Patel, V. K. Yadav, K. K. Yadav, N. Choudhary, H. Kalasariya *et al*., *Water*, **14**, 3163 (2022), https://doi.org/10.3390/w14193163

[12] A. Hadadi, A. Imessaoudene, J.-C. Bollinger, A. A. Assadi, A. Amrane *et al*., *Water*, **14**, 3324 (2022), https://doi.org/10.3390/w14203324

[13] H. A. Mohammed, D. E. Sachit and M. Al-Furaiji, *J. Eng. Sustain. Dev*., **27**, 630 (2023), https://doi.org/10.31272/jeasd.27.5.6

[14] R. Boudraa, D. Talantikite-Touati, A. Souici, A. Djermoune, A. Saidani *et al*., *J. Photochem. Photobiol. Chem*., **443**, 114845 (2023), https://doi.org/10.1016/j.jphotochem.2023.114845

[15] N. A. Abdelwahab and E. M. H. Morsy, *Int. J. Biol. Macromol*., **108**, 1035 (2018), https://doi.org/10.1016/j.ijbiomac.2017.11.021

[16] I. Gasmi, O. Hamdaoui, H. Ferkous and A. Alghyamah, *Ultrason. Sonochem*., **95**, 106361 (2023), https://doi.org/10.1016/j.ultsonch.2023.106361

[17] T. S. Algarni and A. M. Al-Mohaimeed, *J. King Saud University – Science*, **34**, 102339 (2022), https://doi.org/10.1016/j.jksus.2022.102339

[18] Z. Zhang, C. Zhou, J. Yang, B. Yan, J. Liu *et al*., *Sustainability,* **14**, 4082 (2022), https://doi.org/10.3390/su14074082

[19] O. Adam, *Am. Chem. Sci. J*., **16**, 1 (2016), https://doi.org/10.9734/ACSJ/2016/27637

[20] L. Ouettar, E.-K. Guechi, O. Hamdaoui, N. Fertikh, F. Saoudi *et al*., *Molecules*, **28**, 3313 (2023), https://doi.org/10.3390/molecules28083313

[21] J. Escalante, *Renew. Sustain. Energ. Rev*., **169**, 112914 (2022), https://doi.org/10.1016/j.rser.2022.112914

[22] D. Zhong, K. Zeng, J. Li, Y. Qiu, G. Flamant *et al*., *Renew*. *Sustain*. *Energ*. *Rev*., **157**, 111989 (2022), https://doi.org/10.1016/j.rser.2021.111989
[23] B. Janković, N. Manić, V. Dodevski, I. Radović, M. Pijović *et al*., *J*. *Clean*. *Prod*., **236**, 117614 (2019), https://doi.org/10.1016/j.jclepro.2019.117614
[24] K. Benazouz, N. Bouchelkia, A. Imessaoudene, J.-C. Bollinger, A. Amrane *et al*., *Water*, **15**, 3728 (2023), https://doi.org/10.3390/w15213728
[25] Y. S. Al-Degs, M. A. M. Khraisheh, S. J. Allen and M. N. Ahmad, *J*. *Hazard*. *Mater*., **165**, 944 (2009), https://doi.org/10.1016/j.jhazmat.2008.10.081
[26] S. Boumchita, A. Lahrichi, Y. Benjelloun, S. Lairini, V. Nenov *et al*., *J*. *Mater*. *Environ*. *Sci*., **7**, 73 (2016)
[27] F. I. M. S. Sangor and M. A. Al-Ghouti, *Case Stud*. *Chem*. *Environ*. *Eng*., **8**, 100394 (2023), https://doi.org/10.1016/j.cscee.2023.100394
[28] G. Bayramoglu, B. Altintas and M. Y. Arica, *Chem*. *Eng*. *J*., **152**, 339 (2009), https://doi.org/10.1016/j.cej.2009.04.051
[29] L. N. Côrtes, S. P. Druzian, A. F. M. Streit, T. R. Santanna Cadaval Jr., G. C. Collazzo *et al*., *Environ*. *Sci*. *Pollut*. *Res*., **26**, 28574 (2019), https://doi.org/10.1007/s11356-018-3679-2
[30] T. A. Khan, R. Rahman and E. A. Khan, *Earth Syst*. *Environ*., **3**, 38 (2017), https://doi.org/10.1007/s40808-017-0284-1
[31] K. Y. Foo and B. H. Hameed, *Bioresour*. *Technol*., **103**, 398 (2012), https://doi.org/10.1016/j.biortech.2011.09.116
[32] A. Ahmad, M. Rafatullah, O. Sulaiman, M. H. Ibrahim and R. Hashim, *J*. *Hazard*. *Mater*., **170**, 357 (2009), https://doi.org/10.1016/j.jhazmat.2009.04.087
[33] M. Shirani, A. Semnani, H. Haddadi and S. Habibollahi, *Water Air Soil Pollut*., **225**, 2054 (2014), https://doi.org/10.1007/s11270-014-2054-2
[34] R. E. A. Dissanayake, I. M. Premarathne, S. S. Iqbal, N. Priyantha, M. C. M. Iqbal, *Int*. *J*. *Environ*. *Sci*. *Technol*., **19**, 9519 (2022), https://doi.org/10.1007/s13762-021-03711-6
[35] I. Apostol, N. Anghel, F. Doroftei, A. Bele and I. Spiridon, *Mater*. *Today Chem*., **27**, 101299 (2023), https://doi.org/10.1016/j.mtchem.2022.101299
[36] A. F. Dawood and M. A. A. K. Khalil, *Mater*. *Today Proc*., **49**, 2888 (2022), https://doi.org/10.1016/j.matpr.2021.10.221
[37] A. Sayed, G.A. Mahmoud, H. Said and A.A. Diab, *Mater*. *Chem*. *Phys*., **280**, 125731 (2022), https://doi.org/10.1016/j.matchemphys.2022.125731
[38] Y. Zhou, Q. Jin, X. Hu, Q. Zhang and T. Ma, *J*. *Mater*. *Sci*., **47**, 5019 (2012), https://doi.org/10.1007/s10853-012-6378-2